Earth Planets Space, **55**, 427–435, 2003

On the estimates of the ring current injection and decay

P. Ballatore[1] and W. D. Gonzalez[2]

[1]*Istituto di Scienza e Tecnologie dell'Informazione, National Research Council, Via Moruzzi, 1-56124 Pisa, Italy*
[2]*National Institute for Space Research (INPE), Sáo José dos Campos, Brazil*

(Received February 13, 2003; Revised June 23, 2003; Accepted August 7, 2003)

In the context of the space weather predictions, forecasting ring current strength (and of the Dst index) based on the solar wind upstream conditions is of specific interest for predicting the occurrence of geomagnetic storms. In the present paper, we have studied separately its two components: the Dst injection and decay. In particular, we have verified the validity of the Burton's equation for estimating the ring current energy balance using the equatorial electric merging field instead of the original parameter VB_s (V is the solar wind speed and B_s is the southward component of the Interplanetary Magnetic Field, *IMF*). Then, based on this equation, we have used the phase-space method to determine the best-fit approximations for the ring current injection and decay as functions of the equatorial merging electric field (E_m). Results indicate that the interplanetary injection is statistically higher than in previous estimations using VB_s. Specifically, weak but not-null ring current injection can be observed even during northward *IMF*, when previous studies considered it to be always zero. Moreover, results about the ring current decay indicate that the rate of Dst decay is faster than its predictions derived by using VB_s. In addition, smaller quiet time ring current and solar wind pressure corrections are contributing to Dst estimates obtained by E_m instead of VB_s. These effects are compensated, so that the statistical Dst predictions using the equatorial electric merging field or using VB_s are about equivalent.

Key words: Magnetospheric physics, ring current, modeling and forecasting.

1. Introduction

Forecasting the geomagnetic activity and the occurrence of geomagnetic storms are considered as one of the main goals in recent space weather investigations. The most commonly used index of geomagnetic storms is the Dst index. Therefore Dst forecasting has been widely attempted and accurate Dst estimates can be presently computed based on interplanetary space observations (O'Brien and McPherron, 2000a).

The Dst index is derived from the perturbations of the horizontal component of the geomagnetic field as measured by mid-latitude (or latitudes at about 20°–30° from the *CGM*, Corrected GeoMagnetic, equator) ground stations and it is expressed in units nT. It represents the westward ring current formed around the Earth and associated with the occurrence of the geomagnetic storms (Mayaud, 1980; Gonzalez *et al.*, 1994). In particular, the energy of the ring current is carried by energetic ions injected into the magnetosphere powered by the mechanisms of reconnection between the interplanetary magnetic field (*IMF*) and the magnetospheric field. Generally, reconnection occurs when the two fields have opposite directions. At the sub-solar point, this occurs when the *IMF* is directed southward (in the *GSM* coordinate system). Therefore the ring current energy input is considered proportional to the upstream parameter VB_s, where V is the solar wind speed and B_s is the southward *IMF* B_z component (Burton *et al.*, 1975). The original ring current energy balance equation is:

$$\Delta Dst^\star/\Delta t = Q - Dst^\star/\tau \tag{1}$$

where τ is the Dst decay time constant and Q is the ring current energy injection expressed as a linear function of VB_s (Burton *et al.*, 1975). In Eq. (1), $Dst^\star$ represents the Dst corrected by the effects of the solar wind pressure (or the associated magnetospheric currents) and the quiet time ring current

$$Dst^\star = Dst - b\cdot P^{1/2} + c \tag{2}$$

where P is the solar wind pressure and b and c are constants.

A review paper by O'Brien and McPherron (2000a) summarizes and compares previous results about Dst forecasts. The models presented in that paper are based on Eq. (1), which was originally reported by Burton *et al.* (1975). Each model has different parameters Q, τ, b and c in Eqs. (1) and (2). Specifically, O'Brien and McPherron (2000b) considered Q and τ as functions of VB_s and derived b and c (in Eq. (2)) to be 7.26 nT/nPa$^{1/2}$ and 11 nT, respectively. The Q function is different from zero (and in particular it is negative) only for $VB_s > 0.49$ mV/m, when it is:

$$Q[\text{nT/h}] = -4.4\cdot(VB_s[\text{mV/m}] - 0.49). \tag{3}$$

The decay rate, τ, is a function of VB_s and it is:

$$\tau[\text{h}] = 2.4\cdot e^{9.74/(4.69+VB_s[\text{mV/m}])}. \tag{4}$$

Eqs. (3) and (4) give very good Dst forecasts according to Eqs. (1) and (2). Therefore these Q and τ are considered, respectively, as the *effective* ring current interplanetary energy injection and decay. However it might be questioned

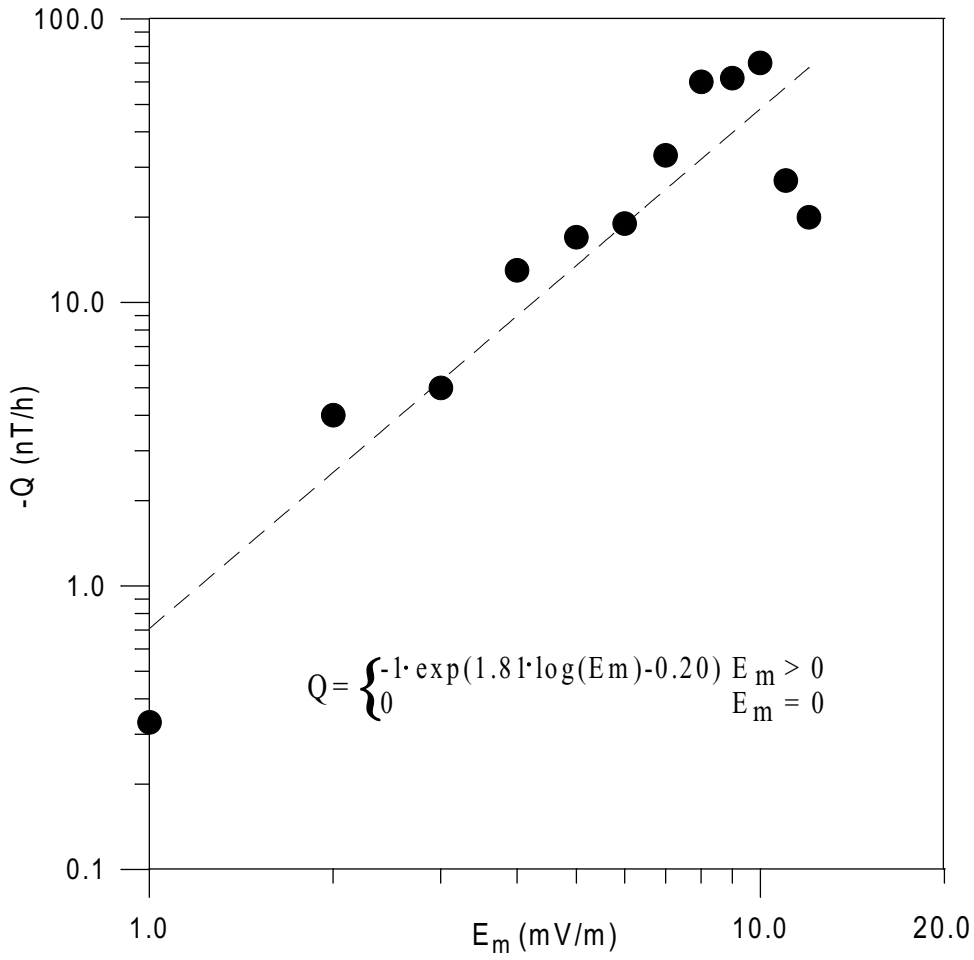

Fig. 1. Injection Q versus E_m. Q values are derived from linear fits to the phase space ΔDst vs. Dst for separate 1 mV/m E_m intervals; each point is shown at the center of the E_m interval to which it refers.

how much these *effective* Q and τ differ from the real ones. In fact it is known that other quantities, besides the VB_s parameter, represent the interplanetary-magnetospheric reconnection. For example, in this paper we consider the equatorial projection of the merging electric field (E_m), which represents the rectified reconnection electric field in the equatorial plane (Gonzalez, 1990). Specifically, the equatorial E_m takes into account effects due to the *IMF* B_y component and the *IMF* clock angle so that contributions from the reconnections at the magnetospheric lobes are taken into account. In particular, E_m coincides with VB_s in the case of clock angle close to 180° or *IMF* $B_y \ll B_z$ with negative B_z.

The equatorial electric field considered here is (Kan and Lee, 1979; Akasofu, 1981):

$$E_m = VB_t \cdot \sin^2(\phi/2) \tag{5}$$

where B_t is the projection of the *IMF* on the *Y-Z* plane (in *GSM* coordinate system) and ϕ is the clock angle between B_t and the Z-axis (Kan and Lee, 1979).

This paper aims to look for the best approximations for the ring current injection and decay as functions of E_m. Conclusions are based on the comparison between the present results and previous findings of Q and τ using VB_s instead of E_m.

2. Data Analysis and Observations

The time interval under investigation is the period since January 1, 1995 until December 31, 2000. For this period, the interplanetary data considered are the measurements of *IMF* components and V from the OMNI/NSSDC database. According to data availability, these measurements are from different satellites, mostly from WIND, but smaller amounts of the data are from IMP-8 and ACE. These measurements have been used to calculate the VB_s and E_m parameters.

A time delay is introduced between the ground based Dst index and the interplanetary data. This delay is chosen equal to 1-h in agreement with previous estimations of average delays between satellites and ground-based measurements (e.g., Ballatore *et al.*, 2001). It is worth mentioning that the 1-h delay is valid statistically, but not exactly at any specific time.

Using Eq. (1), we can calculate the offset and the slope of the linear best-fit for the scatter plots representing ΔDst *vs.* Dst and we can derive Q and τ from the following equations

$$\text{offset} = Q \cdot \Delta t \tag{6}$$

$$\text{slope} = -\Delta t/\tau \tag{7}$$

Considering all the data together, the determination of the offset and slope of the best-fit are not statistically significant due to the large scatter of data. This is in agreement with

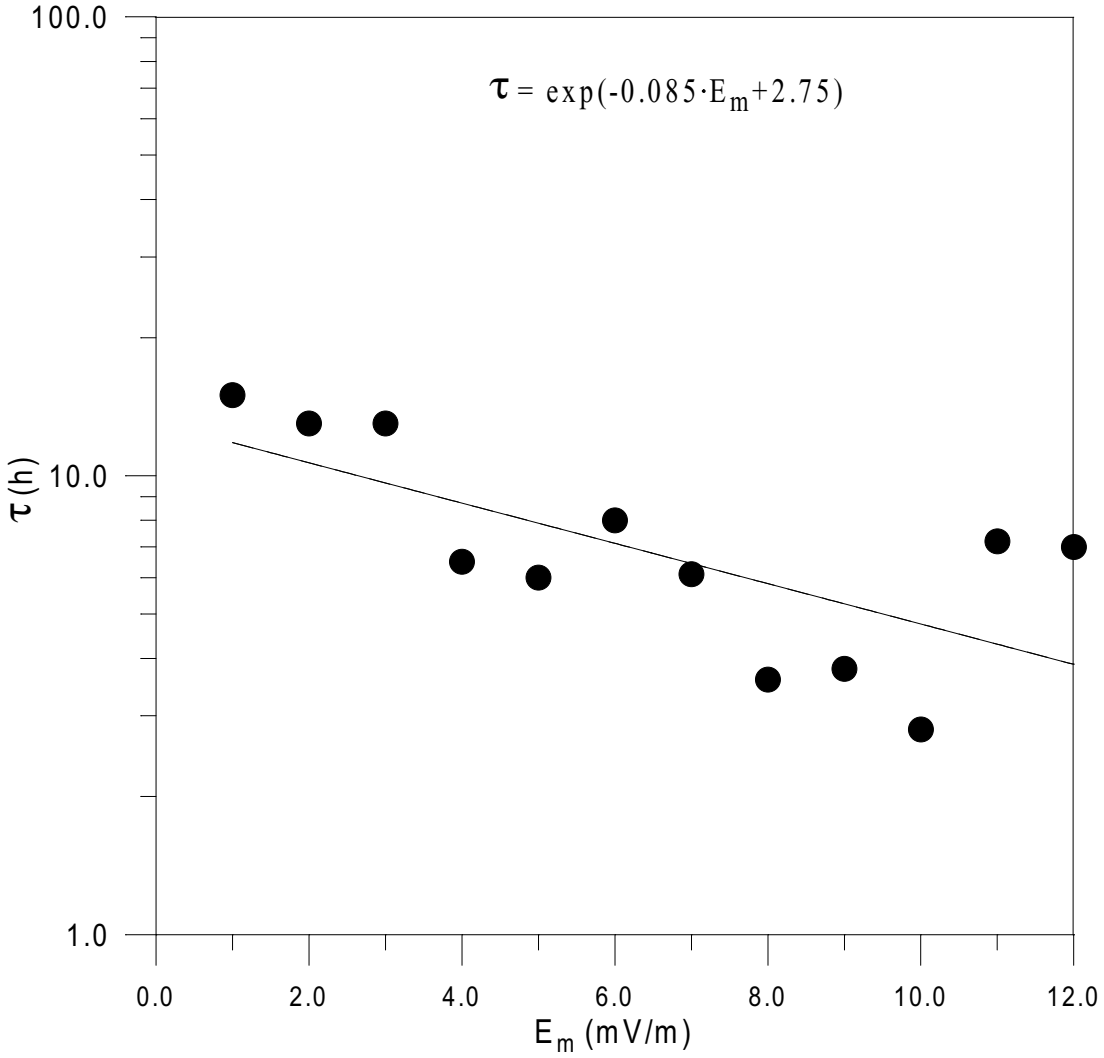

Fig. 2. Decay τ versus E_m. τ values are derived from linear fits to the phase space ΔDst *vs*. Dst for separate 1 mV/m E_m intervals; each point is shown at the center of the E_m interval to which it refers.

the important dependence of Q and τ on the interplanetary parameters (e.g., Fenrich and Luhmann, 1998). However, if each scatter plot is limited only to data points with restricted intervals of VB_s, the best-fits obtained are significant, and Q and τ estimations (from Eq. (6) and Eq. (7)) can be considered statistically significant too. Our procedure here is quite similar to that used by O'Brien and McPherron (2000b).

We have calculated the best-fits for the scatter plots ΔDst *vs*. Dst considering data separated in 1 mV/m intervals of E_m, starting from 0.05 mV/m until 12.5 mV/m. This is similar to the binning for separate VB_s intervals by O'Brien and McPherron (2000b), but they calculated the ΔDst *vs*. Dst best fits in each VB_s sub-set, after having further averaged these data in separate Dst bins. In our case, the linear best-fit correlations take into account each data point measured and are significant at a confidence level above 99.9% until $E_m \sim$ 10.5 mV/m. However, the best correlations are found for the intervals with $E_m < 8$ mV/m, where most of the interplanetary data are observed. Above ∼10.5 mV/m, the confidence level for the best fits are <99.0%, due to the small number of data points involved. The Q and τ derived from Eq. (6) and Eq. (7) are shown in Figs. 1 and 2 as functions of the corresponding E_m (the data points are shown at the center of the 1 mV/m E_m interval to which they refer).

We have studied linear and non-linear fits in Figs. 1 and 2 between Q *vs*. E_m and τ *vs*. E_m, respectively. The best-fits chosen for $Q(E_m)$ and $\tau(E_m)$ (reported on the plots) are the ones corresponding to the best correlation coefficients and the smallest residuals. The correlation coefficients for these two fits are 0.92 in Fig. 1 and 0.76 in Fig. 2 and correspond, respectively, to statistical confidence levels 99.9% and 99.2%. The possibility of defining quite significant best fits can be interpreted as the validity of Burton's equation (Eq. (1)) by using E_m instead of VB_s.

2.1 Ring current injection Q

While the best fit between VB_s and Q is linear (O'Brien and McPherron, 2000b), the best fit between E_m and Q is found to be a power law. This may suggest a strong relationship between the sub-solar point reconnection and the ring current energy input and a quite large magnetospheric/ionospheric re-processing of the ring current energy injection originated by magnetospheric lobe reconnections.

Previously, a similar non-linear relationship was found by Akasofu (1981), between the energy coupling ϵ (ϵ =

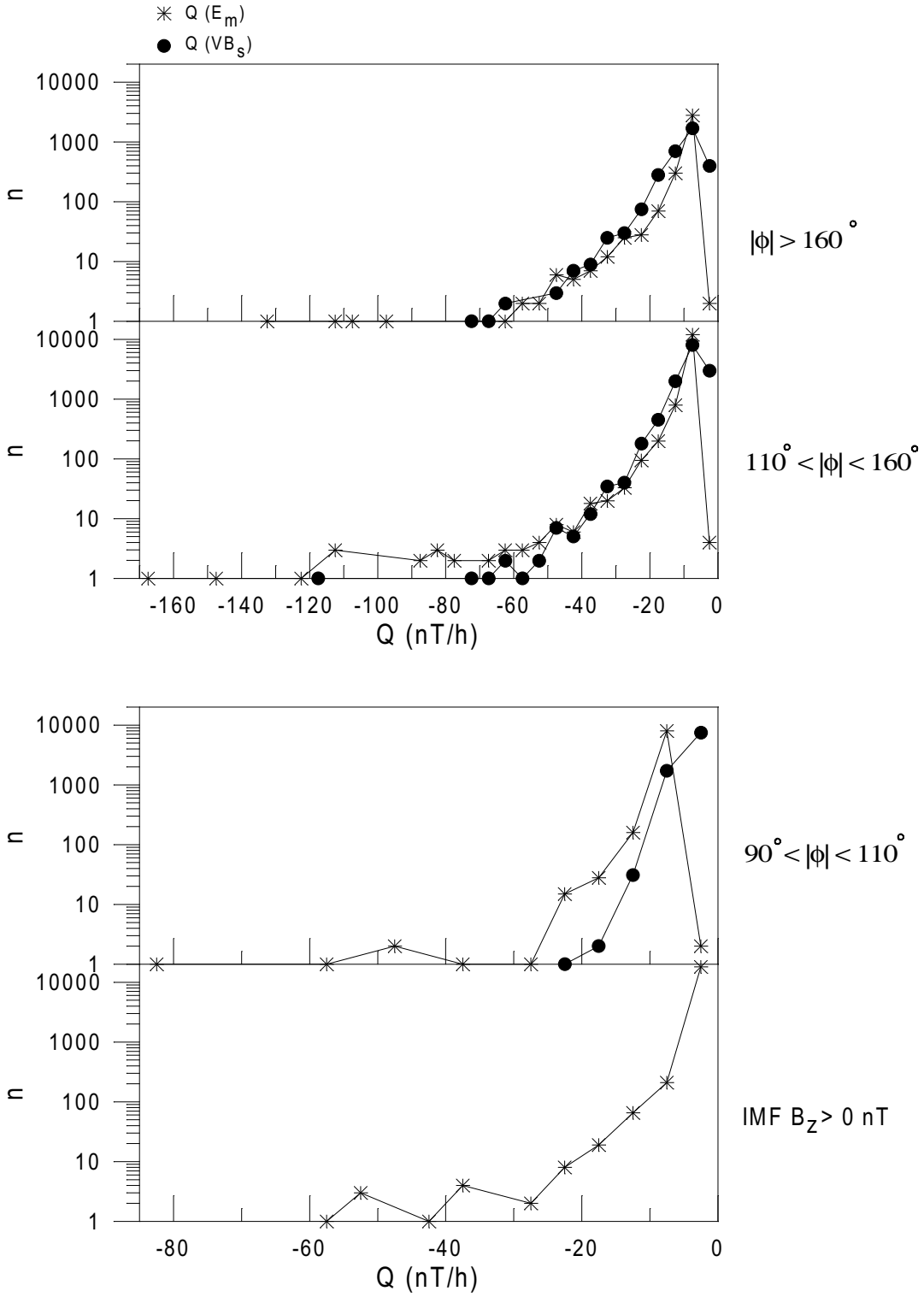

Fig. 3. Number of Q occurrences in the 5 nT/h intervals whose center is indicated on the abscissa. Each panel refers to periods when the clock angle was in the range indicated on the right. The bottom panel refers to periods of *IMF* $B_z > 0$.

$VB^2L^2 \sin^4(\phi/2)$, where B is the module of the total *IMF* vector and L is a scale length at the magnetopause) and the Dst index. In this case, the best-fit was a second order polynomial function in $\log(\epsilon)$f. This was explained by considering that a more intense ring current forms closer to the Earth, where the atmosphere density increases exponentially.

We have studied a quantitative comparison between the function $Q(VB_s)$ calculated according to O'Brien and McPherron (2000b) and the $Q(E_m)$ function given by:

$$\log(-Q(E_m))[\mathrm{nT/h}] = 1.81 \cdot \log(E_m[\mathrm{mV/m}]) - 0.2. \quad (8)$$

Results are shown in Fig. 3, where the number of occurrences of $Q(E_m)$ and $Q(VB_s)$ are reported for separate ranges of the *IMF* clock angle during negative *IMF* B_z (three top panels), and during northward *IMF* (bottom panel). In this figure, each point is illustrated at the center of the 5

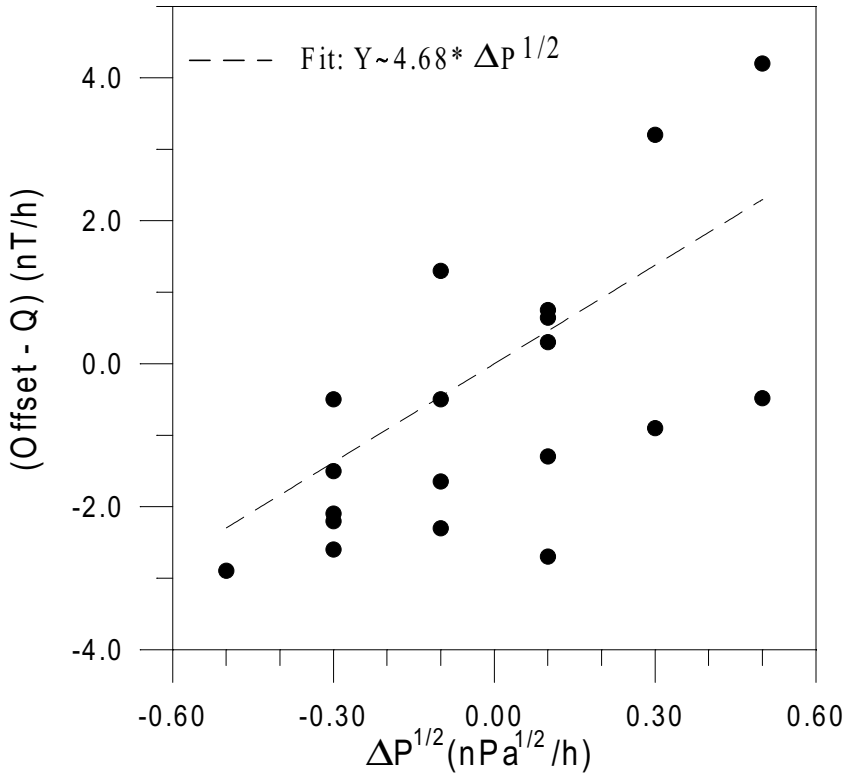

Fig. 4. Residual of phase space offsets minus the injection Q versus variations of the solar wind dynamic pressure P. The constant b in Eq. (2) is estimated by the slope of the fit and it is equal to 4.68.

nT/h Q interval to which it refers. It can be seen that the distribution of $Q(VB_s)$ is clustered at zero, with maximum total occurrence (this total occurrence is the sum of the occurrence in the three upper panels of Fig. 3) in the range between -5 nT/h and 0 nT/h. Differently, the distribution of $Q(E_m)$ is shifted towards higher injection values, with maximum occurrence in the range between -10 nT/h and -5 nT/h for each one of the three upper panels in Fig. 3. The shift between $Q(E_m)$ and $Q(VB_s)$ is especially clear for *IMF* clock angle $|\phi|$ closer to 90°, when the number of occurrences of $Q(E_m)$ is always higher than $Q(VB_s)$ for intervals of $Q < -5$ nT/h.

The bottom panel of Fig. 3 shows the distribution of data points with $Q(E_m)$ different from zero for periods with northward *IMF*, when $Q(VB_s)$ is always equal to zero. Although, in this panel, most of the $Q(E_m)$ occurrences are clustered towards zero, a significant percentage of data lies in the range $(-25, 0)$ nT/h.

2.2 Ring current decay τ

The rate of the ring current decay τ calculated by O'Brien and McPherron (2000b) was based on the hypothesis that an increase in VB_s (i.e., during a higher magnetospheric convection electric field) is associated with a shift towards lower altitudes of the boundary between open and closed drift orbits. At lower altitudes the denser exosphere provides a more rapid charge exchange interactions, resulting in a more rapid decay of the ring current (O'Brien and McPherron, 2000b). In particular, it is assumed that τ is related to the charge exchange lifetime, $\tau \propto (n_H)^{-1}$, where n_H is the density of hydrogen in the geocorona (Smith and Bewtra, 1978). In addition, the geocorona density falls with distance from the Earth, L, as $n_H \propto e^{-L/L_0}$, where L_0 is a scale height determined by atmospheric and gravitational parameters (Smith and Bewtra, 1978). Therefore, O'Brien and McPherron (2000b) considered

$$\tau \propto e^{L/L_0} \tag{9}$$

where L is the distance from the Earth and L_0 is the scale height mentioned above. Considering Φ_0 as the electric field strength proportional to the polar cap potential drop, results by Reiff *et al.* (1981) showed that

$$L^{-1} \propto \Phi_0 \tag{10}$$

And

$$\Phi_0 \propto (a' + VB_s) \tag{11}$$

So that

$$\tau(VB_s)[\mathrm{h}] \propto e^{1/(a'+VBs)}. \tag{12}$$

Equation (12) (O'Brien and McPherron, 2000b) roughly indicates that a decrease in $\tau(VB_s)$ is associated with an increase in VB_s. Similarly, in our case, we find that a decrease in $\tau(E_m)$ is associated with an increase in E_m, with the best functional form given by (see Fig. 2)

$$\log(\tau(E_m)[\mathrm{h}]) = -0.085 \cdot E_m[\mathrm{mV/m}] + 2.75. \tag{13}$$

Our comparison between $\tau(E_m)$ and $\tau(VB_s)$ shows that, for equivalent E_m and VB_s, $\tau(VB_s)$ is generally larger than $\tau(E_m)$, indicating a faster Dst decay associated to $\tau(E_m)$. In fact, for E_m or VB_s in the range $(0, 12)$ mV/m, $\tau(E_m)$ varies in the interval $(14.88, 2.9)$ h while $\tau(VB_s)$ varies in the interval $(17.73, 4.29)$ h.

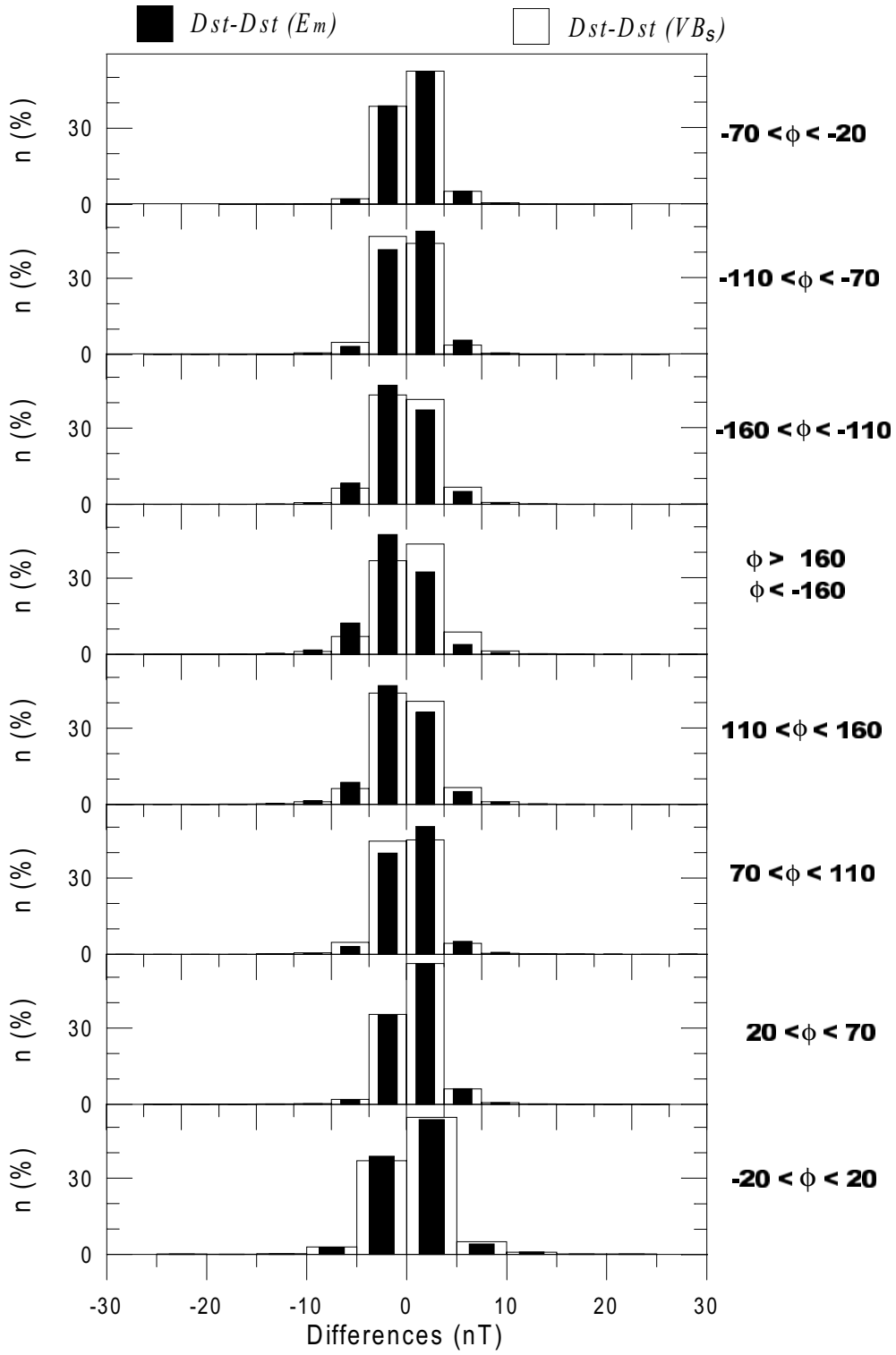

Fig. 5. Distributions of the differences $Dst - Dst(E_m)$ and $Dst - Dst(VB_s)$. Each panel refers to periods when the clock angle lies as indicated at the right of the plot.

2.3 Pressure correction and quiet time ring current

The correction to Dst, introduced in Eq. (1) and related to the solar wind pressure P, takes into account the contribution of the ring current energy balance due to magnetospheric currents (e.g., Burton *et al.*, 1975; O'Brien and McPherron, 2000b). In order to estimate this pressure correction, we use a procedure quite similar to O'Brien and McPherron (2000b). For separate intervals of pressure variations, the differences between the phase space best-fit offsets and $Q(E_m)$ (given by Eq. (8)) are calculated for separate E_m intervals. In each pressure variation range, this is done for each E_m interval in which there is a relatively sufficient number of data points. In this case the definition of the offset given by Eq. (6) is extended to

$$\text{offset} - Q\Delta t = b \cdot \Delta P^{1/2}. \tag{14}$$

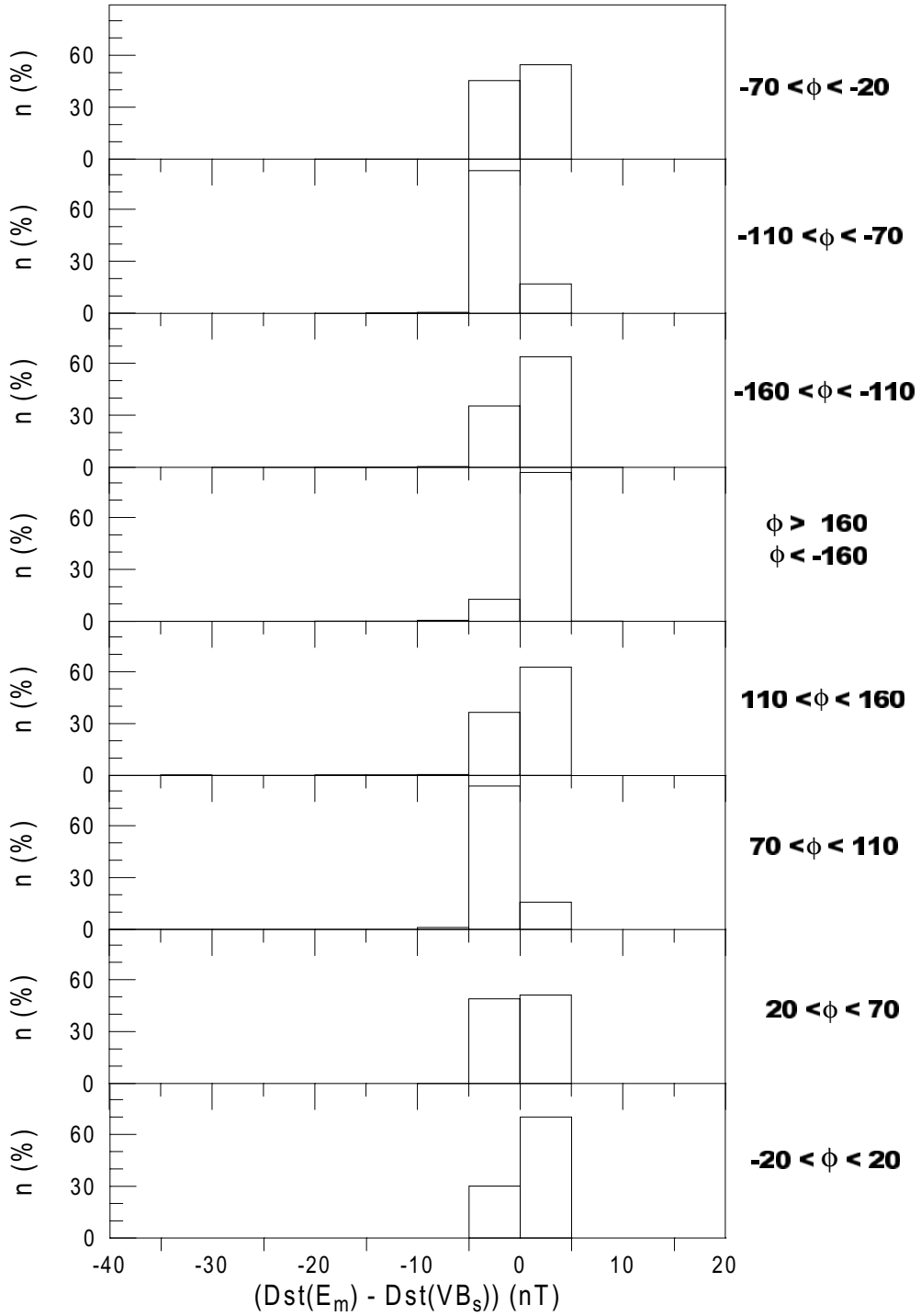

Fig. 6. Distribution of the differences $Dst(E_m) - Dst(VB_s)$. Each panel refers to periods when the clock angle lies as indicated at the right of each plot.

More specifically, 1h data points for the whole period 1995–2000 have been grouped for separate 0.2 $nPa^{1/2}$/h intervals of variation $\Delta P^{1/2}$. Then, separately for each of these groups, a procedure equal to that used for deriving Fig. 1 has been repeated to find the offsets for separate 1 mV/m intervals of E_m. Finally, the differences between these offsets (in units nT/h) and $Q(E_m)$ calculated from Eq. (8) have been found. We show these differences in Fig. 4 as functions of the center of the corresponding 0.2 $nPa^{1/2}$/h interval of $\Delta P^{1/2}$.

From Eq. (14) and the best-fit obtained in Fig. 4, we derive the coefficient b (that corresponds to b given in Eq. (2) and Eq. (14)) as 4.68 nT/$nPa^{1/2}$, which is smaller than the value 7.26 nT/$nPa^{1/2}$ derived using VB_s (O'Brien and McPherron, 2000b). The best fit chosen has a correlation coefficient equal to about 0.64 with 19 data points, corresponding to a statistical confidence level equal to about 99.5%.

To calculate the parameter c of the quiet time ring current correction (given by Eq. (2)), we make use of Eqs. (14) and (15) given by O'Brien and McPherron (2000b) and of the results from Fig. 4. In this way, we obtain a value of c equal to 7.25 nT. Similar to the case of b, our c is smaller than the value 11 nT calculated for VB_s (O'Brien and McPherron,

2000b) and it is also smaller than the original value of 20 nT, derived by Burton *et al.* (1975).

The fact that the estimates of b and c obtained by E_m are smaller than those previously derived by VB_s indicates smaller contributions from magnetopause currents due to the solar wind pressure and smaller level of the quiet time ring current. This might suggest that some of the power previously attributed to these processes is actually driven by *IMF*/magnetosphere reconnections occurring at magnetospheric lobes, which are taken into account by E_m.

2.4 Comparisons among *Dst* and its estimates as functions of VB_s and E_m

The Dst forecast has been computed using interplanetary parameters according to Eq. (1) and the functions $Q(VB_s)$ and $\tau(VB_s)$ given by Eq. (3) and (4). In this way the $Dst(VB_s)$ is calculated as reported by O'Brien and McPherron (2000a, b). Similarly, the $Dst(E_m)$ has been derived by using Eq. (1) with $Q(E_m)$ and $\tau(E_m)$ functions given in Eq. (8) and (13), respectively.

As a further verification of the validity of Eq. (1) for the use of E_m and also to estimate the possible precision of the Dst forecast obtained by E_m, we compared the estimated $Dst(E_m)$ and $Dst(VB_s)$ with the observed Dst index. In Fig. 5 the distributions of the differences $Dst - Dst(E_m)$ and $Dst - Dst(VB_s)$ are reported for separate ranges of the *IMF* clock angle. Both distributions maximize in the range $(-5, 5)$ nT, where a percentage of data points >70% is observed. This indicates good precision of both $Dst(VB_s)$ and $Dst(E_m)$ predictions. In addition, the percentage of occurrences in the range $(-5, 5)$ nT for $Dst(E_m)$ is about the same as the distribution $Dst(VB_s)$. Therefore, the prediction of the ring current level made by E_m can be considered as significant as that made by VB_s. In particular, in Fig. 5, the distributions related to $Dst(E_m)$ and $Dst(VB_s)$ are very much similar for the clock angle ϕ in the range $(-70, 70)^\circ$, namely, during the most northward *IMF* values.

We note that, in Fig. 5, the occurrences of differences in the positive range of the abscissa correspond to the occurrences of a Dst less disturbed than $Dst(E_m)$ or $Dst(VB_s)$, i.e. $Dst(E_m)$ or $Dst(VB_s)$ over-estimates the observed Dst. Similarly, the occurrence of differences in the negative range of the abscissa indicates that the corresponding $Dst(E_m)$ or $Dst(VB_s)$ under-estimates the measured Dst, which is more disturbed. Therefore, Figure 5 shows that, for ϕ around 90°, $Dst(E_m)$ tends to over-estimate the observed Dst, while this is not so for $Dst(VB_s)$. In fact, for ϕ in the interval $(70, 110)^\circ$ and $(-110, -70)^\circ$, the occurrence of $Dst - Dst(E_m)$ is higher in the positive range, while the occurrence of $Dst - Dst(VB_s)$ in the positive range is equal to or smaller than in the negative range. These observations are in agreement with the occurrence of higher merging observed in Fig. 3 for clock angles closer to $|90|^\circ$. On the other hand, for the most southward oriented *IMF* values (ϕ around 180°), $Dst(E_m)$ tends to under-estimate the Dst index, while $Dst(VB_s)$ tends to over-estimate it.

Figure 5 shows that the observed results are rather symmetrical for positive or negative clock angle ranges, so that no significant differences are presently obtained for positive or negative *IMF* B_y periods.

A more direct comparison between $Dst(E_m)$ and $Dst(VB_s)$ is given in Fig. 6, where the distributions of the differences $Dst(E_m) - Dst(VB_s)$ are reported for separate ranges of the *IMF* clock angle. It is shown that $Dst(VB_s)$ tends to indicate a ring current activity higher than $Dst(E_m)$ does, except at clock angles around 90° ($\phi = (-110, -70)^\circ$ and $\phi = (70, 110)^\circ$), when $Dst(E_m)$ is more disturbed. The higher ring current level estimated by $Dst(VB_s)$ than $Dst(E_m)$ is not due to the higher injection $Q(VB_s)$, which is zero during northward *IMF* and tends to be smaller than $Q(E_m)$ also during the other periods (as indicated in Fig. 3). Therefore this higher disturbance indicated by $Dst(VB_s)$ compared with $Dst(E_m)$ can be in part attributed to larger contributions to $Dst(VB_s)$ from the quiet time Dst and from the solar wind pressure correction (Section 2.3) and in part to the fact that $\tau(VB_s)$ is higher than $\tau(E_m)$ (Section 2.2). In particular, these factors seems to compensate the absence of injection for $Dst(VB_s)$ during northward *IMF*. However, the estimates of the ring current injection and decay by E_m are better than that by VB_s. In fact, E_m considers interplanetary-magnetospheric merging as indicated by VB_s and additional magnetospheric-lobe effects (Akasofu, 1981; Gonzalez, 1990).

3. Conclusions

The present study of the ring current energy balance demonstrates the validity of using E_m in predicting Dst (Eq. (1)) (Burton *et al.*, 1975) instead of the parameter VB_s. In fact, the Dst predictions obtained using E_m agree well with the observed Dst. We have given new functional forms for the ring current injection (Q) and decay (τ) in term of E_m.

The estimate of Q as a function of E_m indicates the occurrence of an interplanetary injection greater than that calculated using VB_s. This effect is particularly evident for *IMF* clock angles $|\phi|$ closer to 90°, when the reconnection between the magnetosphere and the interplanetary magnetic field is more active on the magnetospheric lobes. In addition, during positive *IMF* B_z periods, when Q calculated using VB_s is always zero (Burton *et al.*, 1975; O'Brien and McPherron, 2000a, b), the injection estimated using E_m is generally in the range (0, 25) nT.

The prediction of the rate of ring current decay, τ, obtained by using E_m indicates that the real loss should be more rapid than that calculated in previous forecasts. In addition, a smaller level of quiet time ring current and a smaller solar wind pressure correction are obtained using E_m instead of VB_s.

The comparison between Dst predictions produced by VB_s or by E_m shows comparable accuracy. Therefore, we do not promote using E_m instead of VB_s, but we merely highlight that E_m could be alternatively used instead of VB_s in Dst forecasts.

Acknowledgments. The interplanetary data and the geomagnetic index Dst are from the OMNI database, U.S. National Space Science Data Center (NASA, Goddard Space Flight Center, USA).

References

Akasofu, S.-I., Energy coupling between the solar wind and the magneto-

sphere, *Space Sci. Rev.*, **28**, 121–190, 1981.

Ballatore, P., J. P. Villain, N. Vilmer, and M. Pick, The influence of interplanetary medium on SuperDARN scattering occurrence, *Ann. Geophysicae*, **18**, 1576–1583, 2001.

Burton, R. K., R. L. McPherron, and C. T. Russell, An empirical relationship between interplanetary conditions and Dst, *J. Geophys. Res.*, **80**, 4204–4214, 1975.

Fenrich, F. R. and J. G. Luhmann, Geomagnetic response to magnetic clouds of different polarity, *Geophys. Res. Lett.*, **25**, 2999–3002, 1998.

Gonzalez, W. D., A unified view of solar wind—magnetosphere coupling functions, *Planet. Space Sci.*, **38**, 627–632, 1990.

Gonzalez, W. D., J. A. Joselyn, Y. Kamide, H. W. Kroehl, G. Rostoker, B. T. Tsurutani, and V. M. Vasyliunas, What is a geomagnetic storm?, *J. Geophys. Res.*, **99**, 5771–5792, 1994.

Kan, J. R. and L. C. Lee, Energy coupling function and solar wind—magnetosphere dynamo, *Geophys. Res. Lett.*, **6**, 577–580, 1979.

Mayaud, P. N., *Derivation, Meaning and Use of Geomagnetic Indices,* Geophys. Monograph, vol. 22, AGU, Washington, DC, 1980.

O'Brien, T. P. and R. L. McPherron, Forecasting the ring current index Dst in real time, *J.A.S.T.P.*, **62**, 1295–1299, 2000a.

O'Brien, T. P. and R. L. McPherron, An empirical phase space analysis of ring current dynamics: Solar wind control of injection and decay, *J. Geophys. Res.*, **105**, 7707–7720, 2000b.

Reiff, P. H., R. W. Spiro, and T. W. Hill, Dependence of polar cap potential drop on interplanetary parameters, *J. Geophys. Res.*, **86**, 7639–7648, 1981.

Smith, P. H. and N. K. Bewtra, Charge exchange lifetime for ring current ions, *Space Sci. Rev.*, **22**, 301–318, 1978.

P. Ballatore (e-mail: ballatore@isti.cnr.it) and W. D. Gonzalez